Improving Spin-Transport by Disorder

Stanislav Chadov, Janos Kiss, and Claudia Felser*

A new scheme dedicated to improving spin-transport characteristics by applying random disorder as a constructive agent is reported. The approach paves the way for the construction of novel systems with a surprising combination of properties, which are either extremely rare or even entirely absent within the known classes of ordered materials: half-metals with no net magnetization and magnetic semiconductors. As a real case example for the applicability of the scheme, it is shown that a series of such materials can be derived from the tetragonal Heusler compound Mn_3Ga by substituting Mn with a 3d-transition metal.

1. Introduction

In the perspective of contemporary material science, especially within the field of electronic transport, disorder is treated as a severe destructive mechanism, which should be reduced or prevented by all means. In many cases this view is indeed true, which motivates the forgoing search for highly ordered and stable materials and stimulates the optimization of the manufacturing processes. In contrast to this, however, there are several constructive applications of disorder, ranging from simple ones, such as the mechanical reinforcement of steel via defects,[1] roughening the surface of catalysts in order to enhance their activity,[2] the localization of light in photonic crystals,[3] and finally culminating in quantum computers[4] essentially based on exploiting the probabilistic nature of the quantum state. The constructive use of disorder can be straightforwardly applied in band structure engineering as well: the electronic properties connected with a certain group of bands can be enabled or disabled by introducing specific disorder, which selectively affects particular bands, or the rest of the band structure, leaving the selected bands unperturbed.

Due to the fact that spintronics mainly resides on the magneto-resistance (MR) effects,[5] the problem of designing materials with high spin-polarized current remains a permanently vital task. Nowadays, the search for suitable candidate materials is focused mainly on the group of the so-called half-metals,[6,7] because ideally they should conduct electrons exclusively in a single spin-channel. Significant efforts are invested into the identification and synthesis of these materials, as well as into the design of the combined schemes, intended to optimize the characteristics of the whole spintronic devices. However, the actual spin-transport characteristics in real devices often appear to be either too low compared to the theoretical predictions, or they fit acceptably only within a rather narrow range of special conditions.[8–12] Because of these shortcomings, the further improvement of the spin-transport characteristics together with the development of new alternative materials and approaches become undoubtedly important.[13–15]

The spin-polarization of the electric current is defined not only by the spin-polarization of the electrons at the Fermi energy (E_F), but also their spin-resolved mobilities have a crucial role in determining the spin current. Therefore, we will focus on the electronic properties of each spin subsystem separately. In order to offer a clear discussion for the reader, in the following we will denote the ordered half-metals as "M/S" ("metal/semiconductor") due to the metallic character of one spin channel, whereas the other spin channel is semiconducting. By following this nomenclature, we will use the notation of "M/M" ("metal/metal") and "S/S" ("semiconductor/semiconductor") for conventional ordered metals and semiconductors, respectively. In contrast to the vast majority of spintronics-oriented theoretical studies focusing exclusively on the "quantitative" description (i.e., searching for good M/S systems), the present work is essentially based on the "qualitative" manipulation, i.e., on the selective tuning of the mobilities in different spin channels independently from each other. This leads to new unconventional systems, which exhibit very desirable transport properties, similar to the ordered M/S or S/S materials. Still, in contrast to their ordered analogs, their transport properties do not depend on the magnetization, and the electric spin-transport is also independent from the spin-polarization at the E_F. **Figure 1** schematically shows how such systems can be obtained via disorder starting from ordered systems. Upon localizing the electrons in one of the spin-channels of an arbitrary metal (M/M) by disorder we arrive to a system noted as "M/L" (since one spin-channel is mobile, i.e., metallic, and another one is localized) which exhibits spin-transport characteristics similar to conventional M/S (Figure 1a). Furthermore, by localizing the mobile electrons in the metallic spin-channel of an ordered M/S (Figure 1b) we can create an other system type: "L/S" ("localized/semiconductor"). This system exhibits transport properties similar to those of the conventional ordered semiconductors (S/S), but can carry a non-zero magnetic moment.

Dr. S. Chadov, Dr. J. Kiss, Prof. C. Felser
Max-Planck-Institut für Chemische
Physik fester Stoffe
Nöthnitzer Str. 40, 01187 Dresden, Germany
E-mail: stanislav.chadov@cpfs.mpg.de
Dr. S. Chadov, Dr. J. Kiss, Prof. C. Felser
Institut für Anorganische Chemie und Analytische Chemie
Johannes Gutenberg-Universität, 55099 Mainz, Germany

DOI: 10.1002/adfm.201201693

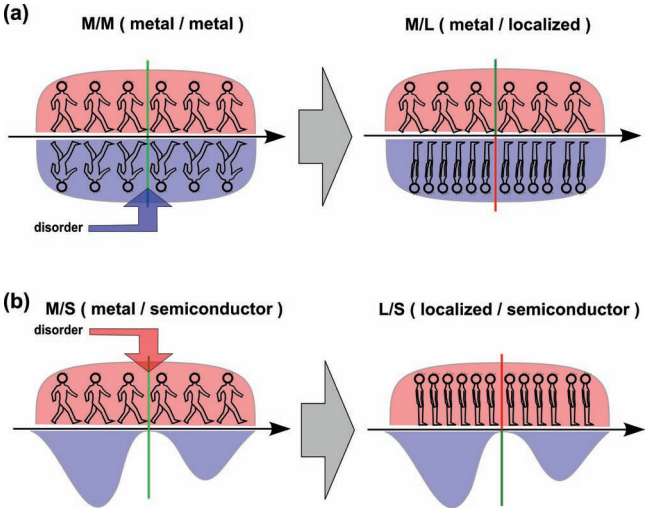

Figure 1. Engineering via disorder in spintronics. Filled light red and blue areas distinguish between the spin-projected DOS in the vicinity of E_F (marked by a vertical line). The electron mobilities in both spin channels are shown schematically as walking (mobile electrons) or standing (localized electrons) people. a) Localization of the carriers by disorder in one of the spin-channels of an arbitrary metal (noted as M/M or "metal/metal") leads to an M/L ("metal/localized") system which produces highly spin-polarized current, similar to conventional ordered half-metals (noted as M/S or "metal/semiconductor"). b) Localization of the carriers by disorder in the metallic spin-channel of the ordered M/S system leads to an L/S ("localized/semiconductor") system in which both spin-channels are blocked: one, by disorder; another one, due to the semiconducting band-gap. From the perspective of electron transport such system behaves as a semiconductor, however they can carry a non-zero magnetic moment.

The electron localization, which is a main underlying mechanism in this design scheme can be easily understood in terms of the Anderson model,[16,17] which states that the spatial localization of an electron is solely defined by the random fluctuations of the potential. This situation is schematically illustrated on **Figure 2**. For the perfect regular crystal shown in Figure 2a the spatial density $\rho(x)$ is lattice-periodic, which can be conveniently represented in the k-space as a countable sum of Bloch waves, depicted as (δ-functions. Since each Bloch $|k\rangle$ -wave infinitely spreads over the whole crystal, the DC (direct current) conductivity is infinite in the case of arbitrary ordered metals. The actual finiteness of the metallic DC conductivity is caused by the translational symmetry break, which is always present in real solids due to diverse degrees of freedom. At low temperatures one of the most efficient sources of localization is provided by chemical disorder. Its mechanism is schematically depicted in Figure 2b, where certain regular lattice position is randomly substituted by another atomic type. This leads to the appearance of localized states with non-periodic spatial density (indicated by the solid green line), which cannot be efficiently represented via a countable Bloch set, but rather requires the continuum of waves (schematically shown as a dense group of green wavy lines). The latter is not possible due to the conservation of the particles number, since each Bloch-state occupies a finite elementary phase volume, fixed by the density of the electrons in the crystal, which implies their countability. For this reason, instead of the sharp δ-like Bloch-states we obtain a set of infinitely spread Lorentzians. Furthermore, even those states, which are not directly affected by disorder turn into Lorentzians, although they still can be very sharp and look as δ-functions due to the finite overlap caused by the interaction of all electronic states.

As it will be demonstrated in the following via ab initio calculations, the outlined mechanisms offer a very powerful engineering tool when they are used in a controlled fashion: the electronic properties connected with a certain group of bands can be enabled or disabled by introducing specific disorder, which selectively affects either these selected bands or the rest of the band structure. In the following we will investigate which parent classes of materials can provide the suitable base for such spin-selective tuning.

2. Results and Discussion

For both scenarios outlined in Figure 1, the appropriate parent systems are those, were E_F is fixed rather stably in one of the spin channels. The manifestation of such stability is the well-known Slater–Pauling behavior of magnetization,[18–20] i.e., the linear scaling of the magnetic moment with the number of valence electrons (exactly as 1 μ_B/electron), observed in the diverse group of cubic Heusler compounds of M/S type. In such systems the

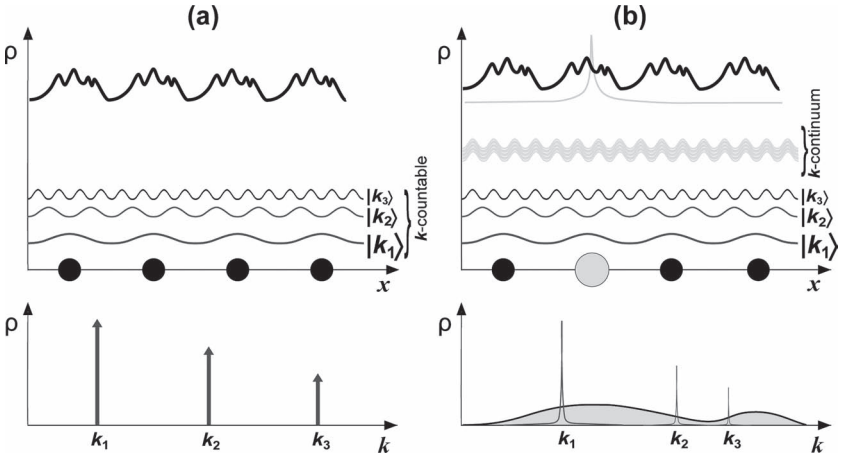

Figure 2. Disorder-induced electron localization. a) Ordered system, with translational-invariant arrangement of atoms (shown as black spheres). The electronic density $\rho(x)$ being a periodic function of the spatial coordinate x (thick solid black line) can be represented via the countable set of delocalized Bloch waves (thinner wavy sine-like lines), each one defined by its k-vector and thus transformed to the reciprocal space as a δ-function. b) Random substitution (light-colored large sphere substitutes one of the regular atoms) gives rise to an additional non-periodic spatially-localized electronic state (shown in light-gray) that cannot be represented by a countable sum of Bloch waves, but rather involves an integration over the k-continuum (manifold of the light-colored wavy lines). Its k-space image will be represented by a long-range delocalized smooth function (light-gray filled area). Due to a finite interaction between all electrons in the system, the former Bloch states, previously seen as δ-peaks, acquire an additional finite broadening as well.

E_F is fixed within the semiconducting band gap, typically exhibited by the minority-spin channel, as was shown in Figure 1b. For this reason, various perturbations (e.g., the variation of the number of valence electrons by substitution) are compensated by the majority-spin channel, which is metallic. Such compounds provide a solid base for the design scheme illustrated in Figure 1b, which is intended to construct the L/S systems. Another class of materials which are good metals in both spin channels, i.e., their spin-polarization of DOS at the E_F is low, but the Fermi energy is still well fixed in one of the spin-channels, are the tetragonally distorted Heusler compounds. These provide an ideal base for the scheme branch outlined in Figure 1a, which illustrates the design of the M/L systems.

To demonstrate the power of the proposed constructive disorder approach, as a practical example we will consider the tetragonally distorted Heusler compound Mn_3Ga as a parent material for the M/L, and, on the other hand, the cubic Mn_2CoGa as a base for the L/S systems. Each of these materials represents an extremely interesting object of research. Mn_3Ga with strong magnetic anisotropy, moderate magnetic moment of 1 μ_B[21] and high Curie temperature of about 780 K[21,22] has drawn much attention as a potential candidate for hard-magnetic[23] and STT-MRAM[24–26] (spin-torque transfer magnetic RAM) applications. Calculations characterize the ordered bulk Mi_2CoGa as a half-metallic system (i.e., M/S) with high spin-polarization at the E_F,[27] having a net magnetic moment of about 2 μ_B[21,28] and a Curie temperature of about 720 K,[21] thus being a good candidate in spintronics. Since these two systems are related by substitution of one Mn atom to Co, we will consider the whole series of $Mn_{3-x}Co_xGa$ alloys ($0 < x < 1$) starting with Mi_3Ga. First, we will demonstrate the appearance of the M/L state within the tetragonal phase (Co-poor regime, $x < 0.5$) and then the appearance of the L/S state within the cubic phase (Co-rich regime, $x > 0.5$).

Ordered Mn_3Ga exhibits a noticeable spin-polarization of DOS at E_F,[29] however it is not a pure half-metal. The latter is caused by the tetragonal Jan-Teller distortion, which splits the in-plane and out-of-plane *d*-orbitals of Mn degenerated at E_F if the system is assumed to be cubic. As it was shown earlier, the hypothetical cubic phase of Mn_3Ga exhibits M/S type properties, and thus almost full spin-polarization at E_F.[30] In reality, the cubic phase undergoes a tetragonal strain, which reduces the unstable high peak of DOS in one of the spin-channels and closes the semiconducting band-gap in the other one, leading to a metal with a moderate spin-polarization of DOS at E_F (M/M). However, for the present purpose the important property of this compound is that due to the tetragonal distortion the E_F is firmly fixed in the DOS minimum of majority-spin channel. The crystal structure and the directions of atomic magnetic moments are shown in **Figure 3**a: the unit cell

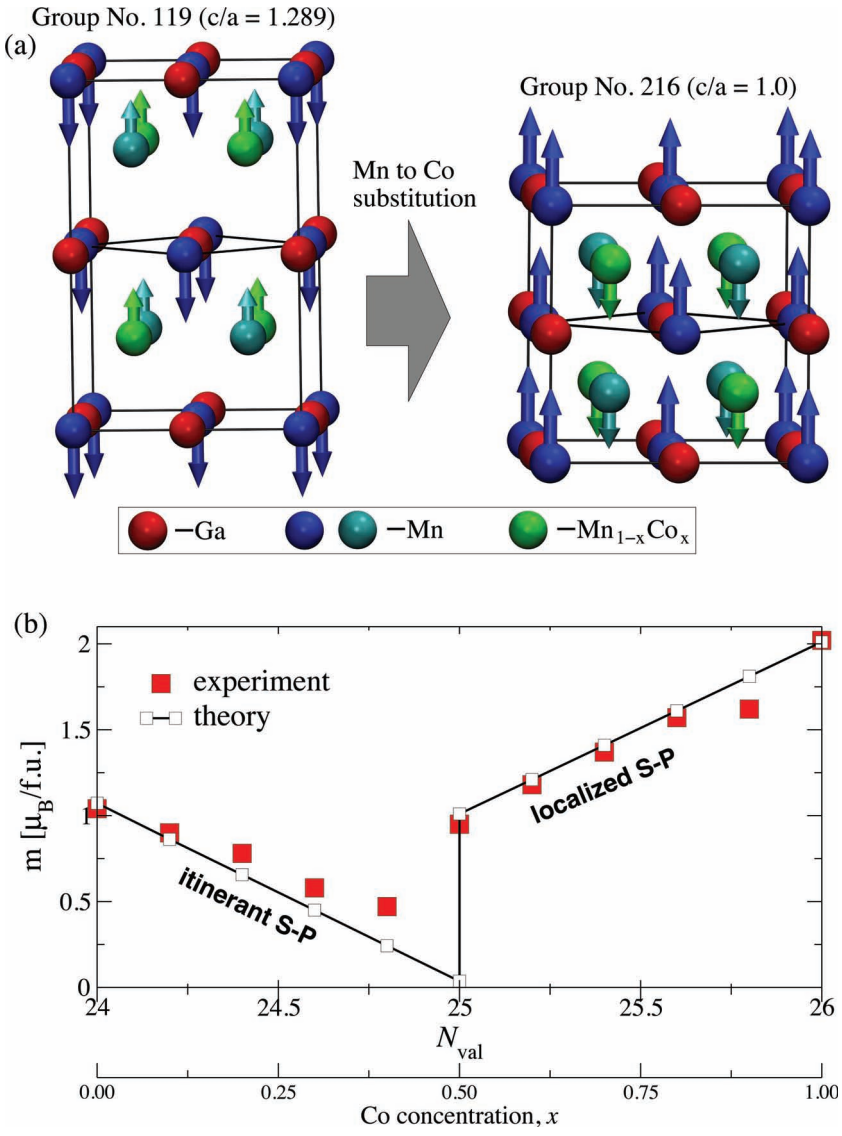

Figure 3. Crystal and magnetic structures of $Mn_{3-x}Co_xGa$ alloys. a) Crystal structures with local magnetic moments. Red spheres mark Ga atoms; dark and light-blue spheres are Mn atoms sitting in two different symmetry positions; sites in which Mn is randomly substituted by Co are marked by green. Arrows indicate the directions of the magnetic moments, which are antiparallel for Mn atoms with different symmetries. The Co-poor series ($x \leq 0.5$) exhibit the strong tetragonal distortion ($c/a \approx 1.29$), whereas the Co-rich ones ($x \geq 0.5$) are cubic. b) Total magnetic moments as a function of the number of valence electrons N_{val} and of the corresponding Co concentrations *x*. Two distinct magnetic regimes refer to the so-called itinerant (magnetic moment decreases with the number of valence electrons) and localized (magnetic moment increases with the number of valence electrons) sides of the Slater–Pauling diagram. Calculated values (marked by open squares connected by solid black line) are compared with experimental data (red squares) taken from ref. [21] The drastic change in the behavior of the magnetic moment at the critical value of Co concentration $x = 0.5$ is due to the tetragonal to cubic structural transformation. Slight increase of the experimental values in the Co-poor regime compared to theory is caused by the certain amount of the cubic phase in the sample, which increases towards $x = 0.5$.

contains two different Mn types with antiparallel alignment of magnetic moments due to different symmetries in lattice positions. Co randomly substitutes one of the two equivalent Mn positions (distinguished for that reason by light-blue and green) which leads to a loss of the inversion symmetry (Group No. 119). The Co-poor series exhibit the so-called itinerant Slater Pauling behavior[20] of the magnetization: it scales down from about 1 μ_B (at $x = 0$) to almost zero ($x = 0.5$) by increasing the number of valence electrons from 24 to 25 (Figure 3b). This indicates that all additional electrons brought by Co fill exclusively the minority-spin channel. At $x = 0.5$ the structure transforms into the cubic phase (Group No. 216). In fact, according to the experimental evidence.[21] close to $x = 0.5$ in Co-poor regime both phases coexist, which is the reason for the small increase of the experimental magnetic moments (shown by big red squares) compared to the ideal calculated values (small open squares, connected by a solid black line). After the system have underwent the phase transition, it remains further cubic within the Co-rich ($x > 0.5$) regime and exhibits the so-called localized Slater–Pauling behavior,[20] i.e., the magnetic moment increases (from 1 to 2 μ_B) with increasing Co content (from $x = 0.5$ to $x = 1$), which clearly indicates its M/S state, which was also shown experimentally.[31]

In our study the atomic positions and lattice parameters were based on experimental structural data.[21] The calculations have been performed using the fully-relativistic Korringa–Kohn–Rostoker (KKR) Green's function method,[32] since it provides a convenient base to describe the random disorder. The latter is treated by means of the so-called CPA (coherent potential aproximation),[33] which is a unique technique to describe the essential features of the electron localization: both energy-dependent shift and the life-time broadening of the electronic states caused by disorder. The exchange-correlation was treated using the Perdew–Burke–Ernzerhof form of the generalized gradient approximation (PBE-GGA).[34] As it follows from Figure 3b, the behavior of the total magnetic moment is well reproduced for the full range of Co concentration in our first-principles calculations. The crucial consequence of the itinerant Slater–Pauling regime for the transport properties is seen immediately by examining the spin-projected band structures and the corresponding DOS. shown on **Figure 4**. The pure Mn_3Ga ($x = 0$) is metallic in both spin-channels, i.e., an M/M-type material with low spin-polarization. The Mn-Co substitution supplies additional electrons exclusively to the minority-spin channel where they become strongly localized, which is seen as broad continuum (Figure 4, $x = 0.5$ case in tetragonal phase). Preferably these extra electrons settle within a sharp minimum of the minority-spin DOS induced by the tetragonal distortion, situated exactly at E_F For this reason the electron localization occurs within the energy window centered at E_F and the conductivity of the minority-spin channel must be severely suppressed. At the same time, the majority-spin channel (shown with red) exhibits well-defined Bloch-like states independently from x. This stability is provided by the deeper majority-DOS minimum, where the E_F gets firmly fixed. This indicates, that the transport properties of the majority-spin channel remain nearly unchanged within the whole Co-poor regime. The most extreme case is provided by the tetragonal structure at the edge of the phase transition at $x = 0.5$, which exhibits an almost zero net magnetic moment and at the same time acquires the maximal degree of the disorder-induced localization, and thus, exhibits drastically different electronic structures in the two

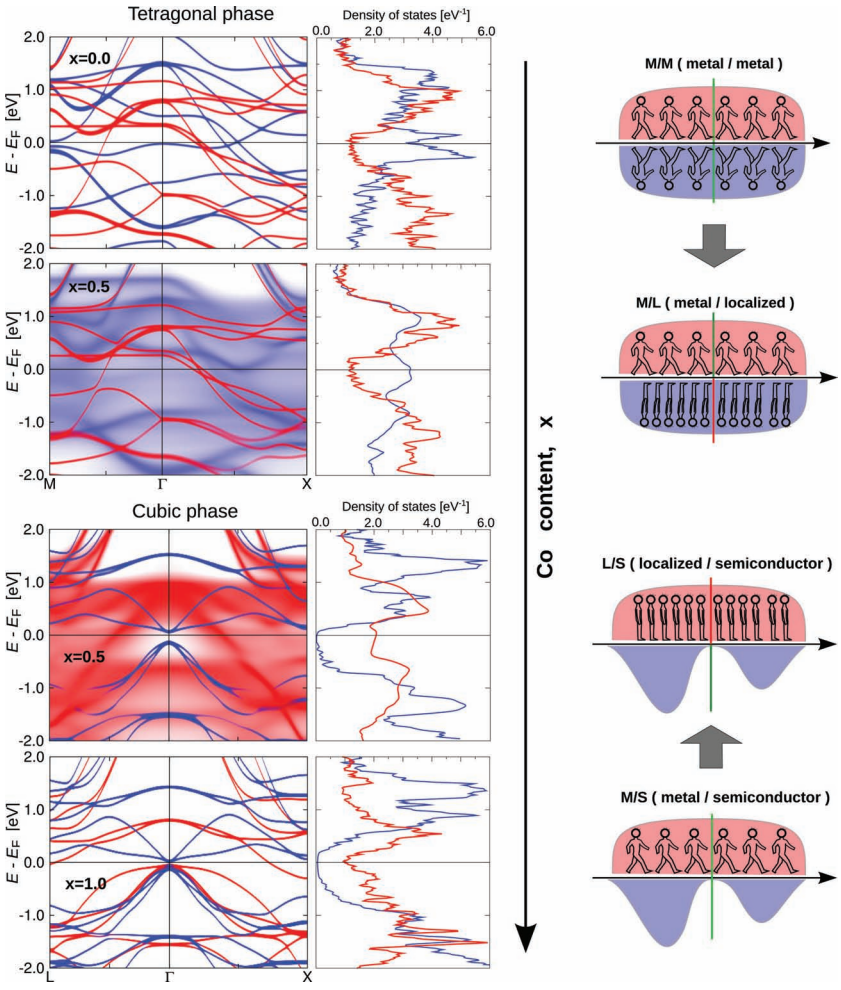

Figure 4. Calculated band structures and DOS of $Mn_{3-x}Co_xGa$ alloys for $x = 0$ (M/M type, tetragonal phase), $x = 0.5$ (M/L type, tetragonal phase), $x = 0.5$ (L/S type, cubic phase) and $x = 1$ (M/S type, cubic phase) compositions together with their schematic type fingerprints (according to Figure 1). Vertical line points towards the increase of Co content x. Red and blue colors correspond to majority- and minority-spin channels, respectively. Within the whole Co-poor regime ($0 \le x \le 0.5$) in which the system is tetragonahy distorted, all modifications caused by Mn-Co substitution are compensated by the minority-spin channel, whereas the majority-spin channel stays almost unaffected. After the transformation into the cubic phase (at $x = 0.5$) the system becomes half-metallic (M/S) and further changes of the band structure are compensated by the majority spin-channel.

spin channels. Such unusual combination of properties is very attractive not only for spin-polarized DC-transport as tunneling or giant magneto-resistance (TMR, GMR) but also for spectroscopic applications involving any type of magnetic dichroism, as e.g., MOKE (magneto-optical Kerr effect) and XMCD or XMLD (X-ray magnetic circular or linear dichroism), etc.

Closer to $x = 0.5$ the minority-spin minimum of DOS at E_F becomes almost filled with Co states and upon further Co substitution it turns into a maximum. This leads to an electron instability, which is relaxed by structural transition into the cubic phase exhibiting typical feature of M/S state: finite DOS at E_F in majority-spin and semiconducting band gap in the minority-spin channel, where E_F will get fixed. This leads to the localized Slater–Pauling behavior, i.e. the increase of the magnetic moment by increasing the number of valence electrons. Thus, the Mn-Co substitution in this regime adds electrons exclusively to the majority-spin channel. Indeed, the latter clearly exhibits a localized character (red-colored smeared bands). In this way we arrive to the L/S state (schematized in Figure 1b), which exhibits transport properties similar to those of conventional semiconductors: the Bloch-like minority-spin channel is gapped, i.e., the DOS of the Bloch carriers is low; the majority-spin channel exhibits a large DOS at E_F but its carriers are localized due to the strong disorder. It is important to point out that by increasing x within the Co-rich regime, the disorder-induced localization in the majority-spin channel (shown with red) becomes weaker (since we move from the most disordered system of $Mn_{2.5}Co_{0.5}Ga$ towards the ordered Mi_2CoGa), but at the same time the majority-spin DOS at E_F decreases (see the red DOS curves for $x = 0.5$ and $x = 1$ in cubic regime). The former mechanism should increase and the latter should decrease the DC conductivity of the majority-spin channel. For this reason one can expect that the transport properties will not substantially change through the whole Co-rich series: i.e., all alloys within the cubic regime represent semiconductor materials, except probably those compositions that are very close to the ordered case, because Mi_2CoGa is typically characterized by the various first-principle calculations[27,35] including the present one, as M/S material.

Finally, as the most essential part of this study, we provide a direct quantitative estimate for these unusual transport characteristics expected from the analysis of the results presented above. To do so, we have employed the general Kubo and Kubo–Středa linear-response formalism,[36,37] which is a state-of-the-art technique, allowing us to calculate the spin-projected DC-conductivities at zero temperature from the first principles. In order to access the spin-resolved components $\sigma^{\uparrow(\downarrow)}$ of the longitudinal conductivity, where the spin projection $\uparrow(\downarrow)$ refers to the z-axis, we have used a relativistic scheme suggested recently[38,37].

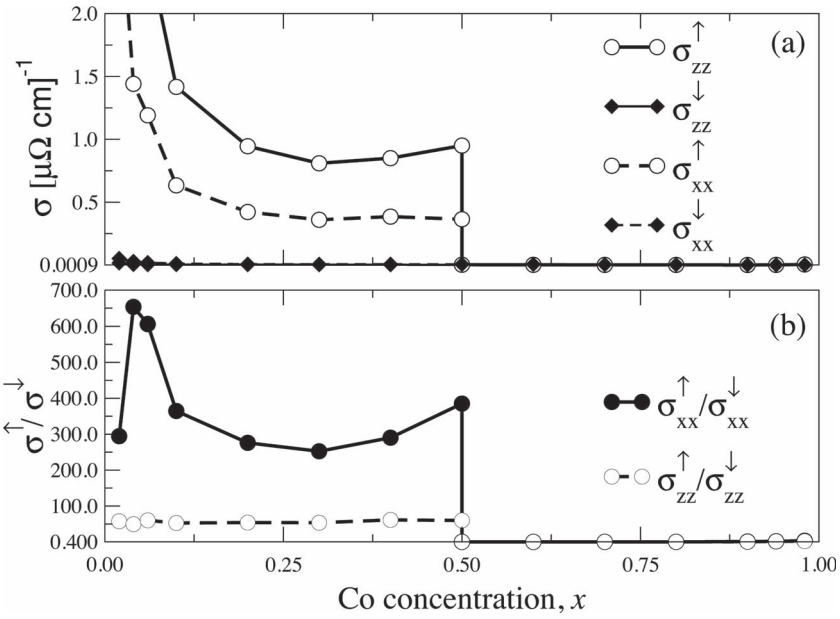

Figure 5. Spin-projected conductivities and their ratios. a) Spin-projected spatial components of the DC conductivity tensor calculated as a function of Co concentration x. Circles and diamonds correspond to majority- ($\sigma^{\uparrow}$) and minority-spin ($\sigma^{\downarrow}$) channels, respectively; solid and dashed lines distinguish between out-of-plane (σ_{zz}) and in-plane (σ_{xx}) spatial components, respectively. In Co-poor regime the minority-spin components affected by disorder are much smaller than majority-spin components ($\sigma^{\uparrow} >> \sigma^{\downarrow}$). This corresponds to the M/L-type systems (see Figure 1). The tetragonal distortion induces a strong transport anisotropy, easily seen as a difference between the majority-spin components ($\sigma_{zz}{}^{\uparrow} \gg \sigma_{xx}{}^{\uparrow}$). In Co-rich regime ($x > 0.5$) both majority- and minority-spin components are small and comparable to each other ($\sigma^{\uparrow}\sigma^{\downarrow} \approx 0.4$): $\sigma^{\uparrow}$ is suppressed by disorder, whereas $\sigma^{\downarrow}$ is small due to the absence of carriers at E_F This corresponds to a systems of L/S-type (see Figure 1). The anisotropy is absent, since in Co-rich regime the structures are cubic. b) Ratios of the spin-projected components: black circles connected by the solid line and open circles connected by the dashed line refer to spatial σ_{zz} and σ_{xx} components, respectively.

The calculated components of the conductivity tensor are shown as a function of Co concentration in **Figure 5**a. In the Co-poor regime both $\sigma^{\uparrow}$ and $\sigma^{\downarrow}$ are suppressed by disorder (at $x = 0$ $\sigma^{\uparrow}$ and $\sigma^{\downarrow}$ are infinite), but the important relation of $\sigma^{\uparrow} \gg \sigma^{\downarrow}$ is kept. Thus, starting from ordered Mi_3Ga, via disordered Mn-Co substitution we arrive to the first system type described in Figure 1, namely the M/L-type. High but finite conductivity of the Bloch-like majority-spin channel (red curves in Figure 1a) indicates that it is affected by disorder indirectly, due to the spin-orbit coupling with the disordered minority-spin channel. Figure 5b shows the ratio of the spin-projected components $\sigma^{\uparrow}/\sigma^{\downarrow}$, which is the central characteristics of the spin-polarization of the electric current. For the in-plane components their mean ratio is about $\sigma_{xx}{}^{\uparrow}/\sigma_{xx}{}^{\downarrow} \approx 60$, whereas in case of the out-of-plane components it is about six times higher, i.e., $\sigma_{zz}{}^{\uparrow}/\sigma_{zz}{}^{\downarrow} \approx 350$ (Figure 5b). This strong anisotropy of the electronic transport is obviously induced by strong spatial anisotropy of the tetragonal geometry. Such high and strongly anisotropic spin-ratios, together with high Curie temperatures suggest the Co-poor tetragonal series to be impressive candidate materials not only for the magneto-resistance itself (TMR, GMR) but also for the anisotropic variants of magneto-resistance (TAMR)[39] and of the magneto-optics as e.g., QMOKE[40] (quadratic MOKE).

The Co-rich regime provides a series of materials with another set of interesting transport properties. As it follows

from Figure 5a,b, for $x > 0.5$ both spin-projected conductivities are small and comparable with each other (Figure 5b). Note, that $\sigma^{\uparrow}/\sigma^{\downarrow} \approx 0.4$ for $x > 0.5$. Due to the cubic form of the crystal at this Co-rich regime, the spatial anisotropy is absent. It is important to note, that both spin-projected conductivities indeed do not substantially change when approaching the clean limit $x = 1$, which agrees with our expectations based on the band structure analysis given above. The minority-spin conductivity $\sigma^{\downarrow}$ stays permanently small, since the corresponding spin-channel is gapped, and this situation holds through almost the whole concentration range (except for pure Mi_2CoGa). Thus, we arrive to the second type of systems schematized in Figure 1, namely to the L/S-type. Here the majority-spin component $\sigma^{\downarrow}$ is suppressed by disorder, which becomes weaker with increasing x, but the DOS at E_F becomes smaller as well, and these two mechanisms compensate one each other. In this way, we obtain a series of semiconductors having a net magnetic moments in the range of 1–2 μ_B.

3. Conclusions

As we have shown, the presented study is interesting both from fundamental scientific view, and from the prospective of industrial applications. Based on our results, the proposed band structure engineering via disorder appears to be a very efficient methodology to manipulate the transport properties by tuning them in different spin channels independently. This uncouples the spin-polarization of current from magnetization and DOS spin-polarization at E_F leading to materials with surprising properties: metals with arbitrary net magnetic moment in the range of 1–2 μ_B which generate highly spin-polarized current, and magnetic semiconductors with moments of 1–2 μ_B. Further studies on these materials are of great interest, in particular experimental investigations involving various types of spin-asymmetry measurements.

Although the design scheme introduced in this work was demonstrated only for Mn_3Ga and Mi_2CoGa parent compounds, we are confident that its potential applicability is rather broad. As it follows from the analysis presented above, an important indication for the M/L-type candidates is the itinerant regime of their Slater–Pauling behavior, caused by stabilization of E_F in the pronounced minimum of the majority-spin DOS. Since the group of the tetragonally-distorted Heusler compounds has become a hot research topic rather recently (hard magnets, STT-MRAM, shape-memory alloys), at present this family is still much less studied compared to the cubic Heusler alloys. Thus, currently, a promising material base for the M/L-type systems are the series generated by Mn-X substitution (with X being a transition metal, e.g., Fe or Ni) in parent compounds of Mn_3Z type (where Z is a main-group element, e.g., Ga or Sn). Also, it is worth to mention the Mn-poor alloy series as well, such as $Mn_{3-x}Ga$ ($0 < x < 1$), which where extensively studied as a promising STT-MRAM material,[29,41,42] Another candidate subgroup can be provided by the transition-metal binary alloys (e.g., FeCo, CoCr, FeNi) exhibiting the itinerant Slater–Pauling behavior as well. The L/S-type systems can be obtained in a more simple way: they can be based on the ordered half-metallic materials exhibiting the localized Slater–Pauling behavior (including the semiconductors as a partial case of the half-metals). These systems are provided by the rich family of the cubic Heusler compounds (altogether more than 1000 known members). Since the electronic localization can be achieved more efficiently in low-dimensional systems, it is promising to study the transport properties of the proposed materials, both M/L and L/S, in form of thin films as well.

From a fundamental perspective these type of studies are also extremely attractive, since they require a very detailed understanding of the disorder mechanisms. Obviously there are many other potential sources of disorder (e.g., structural or magnetic), which can be used in the band structure engineering of new materials. In addition, this topic is inherently connected with an extreme limit of the electron localization, i.e., the so-called Anderson localization, when the electrons cannot move even in a diffusive way, since the length of their mean-free path becomes shorter than the de Broglie wavelength. The question whether the CPA approach is able to describe such extreme localization remains a subject of vivid debates.[43–49] In turn, this renews the interest towards the more sophisticated mean-field theories, as non-local extensions of CPA,[50–52] which greatly extend the applicability of the first-principle calculation schemes.

Acknowledgements

The authors would like to thank Jürgen Kübler for his criticism and helpful suggestions. Financial support by the DFG project FOR 1464 "ASPIMATT" (1.2-A) is gratefully acknowledged.

Received: June 22, 2012
Published online: September 25, 2012

[1] W. Soboyejo, *Mechanical properties of engineered materials*, CRC Press, New York **2002**.
[2] B. L. M. Hendriksen, M. D. Ackermann, R. van Rijn, D. Stoltz, I. Popa, O. Balmes, A. Resta, D. Wermeille, R. Felici, S. Ferrer, J. W. M. Frenken, *Nat. Chem.* **2010**, *2*, 730–734.
[3] L. Sapienza, H. Thyrrestrup, S. Stobbe, P. D. Garcia, S. Smolka, P. Lodahl, *Science* **2010**, *327*, 1352–1355.
[4] J. Brown, *New Sci.* **1994**, *133*, 21–24.
[5] I. Žutić, J. Fabian, S. D. Sarma, *Rev. Mod. Phys.* **2004**, *76*, 323–410.
[6] J. Kübler, A. R. Williams, C. B. Sommers, *Phys. Rev. B* **1983**, *28*, 1745–1755.
[7] R. A. de Groot, F. M. Mueller, P. G. van Engen, K. H. J. Buschow, *Phys. Rev. Lett.* **1983**, *50*, 2024.
[8] J. Schmalhorst, S. Kämmerer, M. Sacher, G. Reiss, A. Hiitten, A. Scholl, *Phys. Rev. B* **2004**, *70*, 024426–024432.
[9] N. D. Telling, P. S. Keatley, G. van der Laan, R. J. Hicken, E. Arenholz, Y. Sakuraba, M. Oogane, Y. Ando, T. Miyazaki, *Phys. Rev. B* **2006**, *74*, 224439–224445.
[10] M. Lezaic, P. Mavropoulos, J. Enkovaara, G. Bihlmayer, S. S Blügel, *Phys. Rev. Lett.* **2006**, *97*, 026404.
[11] J. J. Attema, G. A. de Wijs, R. A. de Groot, *J. Phys. D: Appl. Phys.* **2006**, *39*, 793.
[12] V. Ko, J. Qiu, P. Luo, G. C. Han, Y. P. Feng, *J. Appl. Physics* **2011**, *109*, 07B103.
[13] S. Chadov, T. Graf, K. Chadova, X. Dai, F. Casper, G. H. Fecher, C. Felser, *Phys. Rev. Lett.* **2011**, *107*, 047202.
[14] J. Ma, J. Hu, Z. Li, C.-W. Nan, *Adv. Mater.* **2011**, *23*, 1062–1087.
[15] X. Hu, *Adv. Mater.* **2012**, *24*, 294–298.

[16] P. W. Anderson, *Phys. Rev.* **1958**, *109*, 1492–1505.
[17] D. J. Thouless, *Phys. Rep. C* **1974**, *13*, 93–142.
[18] J. C. Slater, *Phys. Rev.* **1936**, *49*, 931–937.
[19] L. Pauling, *Phys. Rev.* **1938**, *54*, 899–904.
[20] J. Kübler, *Phys. B* **1984**, *127*, 257–263.
[21] V. Alijani, J. Winterlik, G. H. Fecher, C. Felser, *Appl. Phys. Lett.* **2011**, *99*, 222510.
[22] B. Balke, G. H. Fecher, J. Winterlik, C. Felser, *Appl. Phys. Lett.* **2007**, *90*, 152504.
[23] J. M. D. Coey, *IEEE Trans. Magn.: Adv. Magn.* **2011**, *47*, 4671–4681.
[24] L. Berger, *Phys. Rev. B* **1996**, *54*, 9353–9358.
[25] J. C. Slonczewski, *J. Magn. Magn. Mater.* **1996**, *159*, L1–L7.
[26] W. J. Gallagher, S. S. P. Parkin, *IBM J. Res. Dev.– Spintronics* **2006**, *50*, 5–23.
[27] K. Özdogan, I. Galanakis, E. Şaşioglu, B. Aktas, *Solid State Commun.* **2007**, *142*, 492–497.
[28] M. Meinert, J.-M. Schmalhorst, C. Klewe, G. Reiss, E. Arenholz, T. Böhnert, K. Nielsch, *Phys. Rev. B* **2011**, *84*, 132405.
[29] J. Winterlik, B. Balke, G. H. Fecher, C. Felser, M. C. M. Alves, F. Bernardi, J. Morais, *Phys. Rev. B* **2008**, *77*, 054406.
[30] S. Wurmehl, H. C. Kandpal, G. H. Fecher, C. Felser, *J. Phys.: Condens. Matter* **2006**, *18*, 6171–6181.
[31] P. Klaer, C. A. Jenkins, V. Alijani, J. Winterlik, B. Balke, C. Felser, H. J. Elmers, *Appl. Phys. Lett.* **2011**, *98*, 212510.
[32] H. Ebert, D. Ködderitzsch, J. Minár, *Rep. Prog. Phys.* **2011**, *74*, 096501.
[33] P. Soven, *Phys. Rev.* **1967**, *156*, 809–813.
[34] J. P. Perdew, K. Burke, M. Ernzerhof, *Phys. Rev. Lett.* **1996**, *77*, 3865–3868.
[35] N. Xing, H. Li, J. Dong, R. Long, C. Zhang, *Comp. Mater. Sci.* **2008**, *42*, 600–605.
[36] W. H. Butler, *Phys. Rev. B* **1985**, *31*, 3260–3277.
[37] S. Lowitzer, M. Gradhand, D. Ködderitzsch, D. V. Fedorov, I. Mertig, H. Ebert, *Phys. Rev. Lett.* **2011**, *106*, 056601.
[38] A. Vernes, B. L. Györffy, P. Weinberger, *Phys. Rev. B* **2007**, *76*, 012408.
[39] C. Gould, K. Pappert, G. Schmidt, L. Molenkamp, *Adv. Mater.* **2007**, *19*, 323–340.
[40] J. Hamrle, S. Blomeier, O. Gaier, B. Hillebrands, H. Schneider, G. Jakob, K. Postava, C. Felser, *J. Phys. D: Appl. Phys.* **2007**, *40*, 1563–1569.
[41] W. Feng, D. D. Dung, Y. Shin, D. V. Thiet, S. Cho, X. Hao, *J. Korean Phys. Soc.* **2010**, *56*, 1382–1386.
[42] H. Kurt, K. Rode, M. Venkatesan, P. Stamenov, J. M. D. Coey, *Phys. Status Solidi B* **2011**, *248*, 2338–2344.
[43] E. N. Economou, M. H. Cohen, *Phys. Rev. B* **1972**, *5*, 2931–2948.
[44] R. Harris, M. Plischke, *Solid State Commun.* **1972**, *11*, 1165–1168.
[45] A. R. Bishop, *Philos. Mag.* **1973**, *27*, 651–664.
[46] E. Kolley, W. Kolley, *Z. Phys. B* **1986**, *65*, 7–14.
[47] J. Kroha, C. M. Soukoulis, P. Wölfle, *Phys. Rev. B* **1993**, *47*, 11093–11096.
[48] C. M. Soukoulis, E. N. Economou, *Waves Random Media* **1999**, *9*, 255–269.
[49] M. Laad, L. Craco, *J. Phys.: Condens. Matter* **2005**, *17*, 4765–4777.
[50] A. Mookerjee, V. K. Srivastavat, V. Choudhry, *J. Phys. C: Solid State Phys.* **1983**, *16*, 4555–4564.
[51] C. I. Ventura, R. A. Barrio, *Physica B* **2000**, *281–282*, 855–856.
[52] D. A. Rowlands, J. B. Staunton, B. L. Györffy, *Phys. Rev. B* **2003**, *67*, 115109.